Synthesis and Photophysical Characteristics of 2,7-Fluorenevinylene-Based Trimers and Their Electroluminescence

ARTICLE *in* THE JOURNAL OF PHYSICAL CHEMISTRY B · NOVEMBER 2006

Impact Factor: 3.3 · DOI: 10.1021/jp0631477 · Source: PubMed

3 AUTHORS:

John A Mikroyannidis
University of Patras
277 PUBLICATIONS **3,816** CITATIONS
SEE PROFILE

Larysa Fenenko
16 PUBLICATIONS **162** CITATIONS
SEE PROFILE

Chihaya Adachi
Kyushu University
364 PUBLICATIONS **15,633** CITATIONS
SEE PROFILE

Synthesis and Photophysical Characteristics of 2,7-Fluorenevinylene-Based Trimers and Their Electroluminescence

John A. Mikroyannidis,*,† Larysa Fenenko,‡ and Chihaya Adachi‡

Chemical Technology Laboratory, Department of Chemistry, University of Patras, GR-26500 Patras, Greece, and Center for Future Chemistry, Kyushu University, 744 Motooka, Nishi, Fukuoka 819-0395, Japan

Received: May 23, 2006; In Final Form: July 11, 2006

Three new 2,7-fluorenevinylene-based trimers were synthesized and characterized. The synthesis was carried out by the Heck coupling reaction of 9,9-dihexyl-2,7-divinylfluorene with 2-(4-bromophenyl)-5-phenyl-1,3,4-oxadiazole, *N*,*N*-diphenyl-4-bromoaniline, or 3-bromopyrene to afford the trimers **OXD**, **TPA**, and **PYR**, respectively. All the trimers were readily soluble in common organic solvents such as tetrahydrofuran, dichloromethane, chloroform, and toluene. Their glass transition temperatures ranged from 33 to 60 °C. The UV−vis spectra showed an absorption maximum at $\lambda_{a,max} = 379-417$ nm with optical band gap of $E_g = 2.47-2.66$ eV. In solution, they emitted strong blue-green photoluminescence (PL) with PL maximum at $\lambda_{f,max} = 455-565$ nm and fluorescence quantum yield of $\Phi_f = 0.65-0.74$. On the other hand, in their spin-coated films, the PL efficiencies significantly decreased due to the presence of concentration quenching. All samples showed nanosecond transient lifetime containing two components, suggesting excimer formation. The organic light-emitting diodes (OLEDs) with **OXD** and **TPA** showed green emission with electroluminescence (EL) quantum efficiencies of $\eta_{EL} \sim 10^{-2}$%, while very weak EL efficiency of $\eta_{EL} \sim 10^{-5}$% was observed with PYR. The highest occupied molecular orbital (HOMO) levels of the films were found to be 5.05−5.75 eV.

Introduction

Conjugated organic oligomers and polymers have reached the role of a major, technologically important class of materials. Conjugated organic polymers have the advantages of low cost, ease of modification of properties by appropriate substitution, and solvent processability. Major applications include the development of electronic devices such as field-effect transistors,[1−3] solar cells,[4,5] and organic light-emitting diodes (OLEDs).[6−10] Oligomers are of particular interest because they generally possess good molecular-ordering properties when processed using vacuum-sublimation techniques. Moreover, they have the capability to be soluble in organic solvents with the introduction of proper chemical substituents. Recently, the synthesis of various well-defined conjugated oligomers and polymers derived from phenylene, pyrrole, thiophene, and fluorene moieties has been achieved. However, the fabrication of novel materials for future electronic devices from conjugated building blocks is still a challenge.

For over a decade, poly(*p*-phenylenevinylenes) (PPVs), have been the subject of investigations aimed toward their application in electroluminescent devices such as OLEDs;[10] they constitute one of the most studied families of conjugated polymers.[11] More recently, poly(fluorenes) have received increased attention[12−22] as a class of electroluminescent conjugated polymers for blue light-emitting diodes due to their high photoluminescent quantum yields in the solid state and good charge transport properties.[23] Of these, most effort was directed toward poly(9,9-dioctylfluorene) and poly(9,9-dihexylfluorene). They show high fluorescence efficiencies in the solid state, can be readily processed from solution, form high-quality thin films, and emit in the desirable blue region of the spectrum. Unfortunately, it has been shown that these materials undergo irreversible changes in the emission spectra on device operation unless the starting monomers are rigorously purified to remove any fluorene units that carry a labile H atom in the 9-position.[24] In these experiments the desirable blue emission of the pristine polymer is rapidly transformed to a lower energy blue-green emission.[25−27]

2,5-Diaryl-1,3,4-oxadiazole derivatives are electron-deficient systems which possess good thermal and chemical stabilities as well as high photoluminescence quantum yields.[28,29] This combination of properties has led to their use as electron-transporting materials in OLEDs.[29,30] On the other hand, the triphenylamine derivative is well-known as a typical hole-transporting material and has a hole mobility of 10^{-3} to 10^{-5} $cm^2/(V\ s)$.[31,32] Finally, pyrene has been extensively used for the investigation of water soluble polymers. Among the most attractive features of pyrene are its well-characterized long-lived excited state, the sensitivity of its fluorescence to quenching, the sensitivity of its excitation spectra to microenvironment changes, and its propensity for forming excimers.[33] A literature survey revealed that there are a limited number of investigations concerning the attachment of pyrene to polymers.[34] Pyrene-containing polymers have been used as acceptors for energy transfer from various donors.[35] Recently, we prepared a series of random co-polyfluorenes containing pyrenyltriazine segments.[36] Furthermore, we prepared a luminescent monomer of substituted tetrastyrylpyrene and a PPV derivative with pyrene segments along the backbone.[37]

In the context of the present investigation, three new 2,7-fluorenevinylene trimers were successfully synthesized via the Heck coupling reaction. They contained a central 2,7-fluorene-

* To whom correspondence should be addressed. E-mail: mikroyan@chemistry.upatras.gr.
† University of Patras.
‡ Kyushu University.

10.1021/jp0631477 CCC: $33.50
Published on Web 09/16/2006

CHART 1

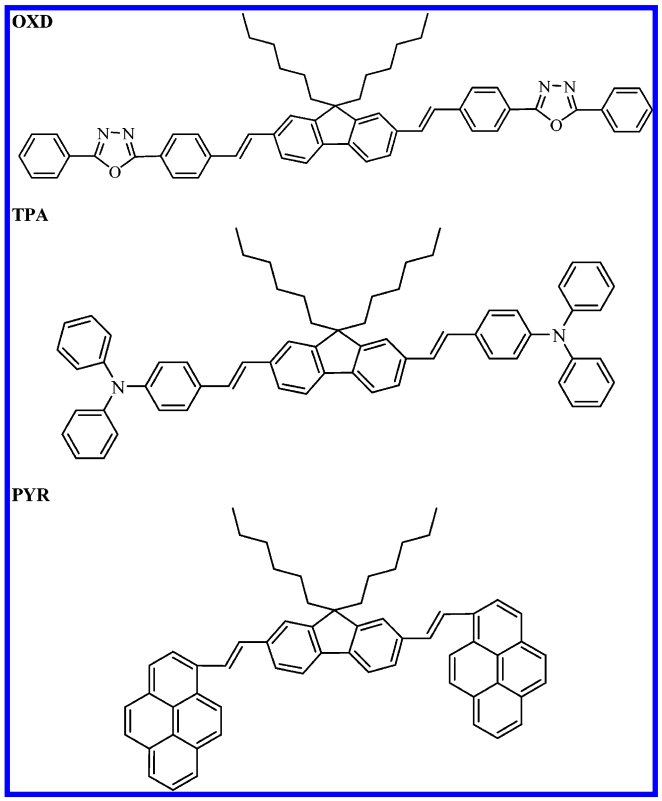

vinylene segment to which a substituent (trimer structures are identified by the respective substituent, **OXD**, **TPA**, or **PYR**) with various chemical structures was attached at both sides. This substituent was a derivative of 2,5-diphenyl-1,3,4-oxadiazole, triphenylamine, or pyrene. The oxadiazole and triphenylamine units are expected to improve the electron- and hole-transport properties of the trimers, respectively. On the other hand, pyrene is a strongly luminescent group with interesting features. The two hexyl chains at the C-9 of fluorene enhanced the solubility of the trimers. The photophysical and electroluminescent properties of these trimers were systematically investigated.

Experimental Section

Characterization Methods. IR spectra were recorded on a Perkin-Elmer 16PC FT-IR spectrometer with KBr pellets. ^{1}H NMR (400 MHz) and ^{13}C NMR (100 MHz) spectra were obtained using a Brucker spectrometer. Chemical shifts (δ values) are given in parts per million with tetramethylsilane as an internal standard. UV−vis spectra were recorded on a Beckman DU-640 spectrometer with spectrograde tetrahydrofuran (THF). The photoluminescence (PL) spectra were obtained with a Perkin-Elmer LS45 luminescence spectrometer. The PL spectra were recorded with the corresponding excitation maximum as the excitation wavelength. Thermogravimetric analysis (TGA) was performed on a DuPont 990 thermal analyzer system. Ground trimer samples of about 10 mg each were examined by TGA, and the weight loss comparisons were made between comparable specimens. Dynamic TGA measurements were made at a heating rate of 20 °C/min in atmospheres of N_2 at a flow rate of 60 cm^3/min. Thermomechanical analysis (TMA) was recorded on a DuPont 943 TMA using a loaded penetration probe at a scan rate of 10°C/min in N_2 with a flow rate of 60 cm^3/min. The TMA experiments were conducted at least in duplicate to ensure the accuracy of the results. The TMA specimens were pellets of 10 mm diameter and ∼1 mm thickness prepared by pressing powder of the polymer for 3 min under 8 kp/cm^2 at ambient temperature. The T_g is assigned by the first inflection point in the TMA curve, and it was obtained from the onset temperature of this transition during the second heating. Elemental analyses were carried out with a Carlo Erba model EA1108 analyzer.

To measure the PL quantum yields (Φ_f), degassed solutions of the trimers in THF were prepared. The concentration was adjusted so that the absorbance of the solution would be lower than 0.1. The excitation was performed at the corresponding excitation maximum, and a solution in 1 N H_2SO_4 of quinine sulfate, which has $\Phi_f = 0.546$, was used as a standard.

To investigate photophysical properties of **OXD**, **TPA**, and **PYR** in their thin films, they were spin-coated from 1 wt % solutions in dichloromethane (DCM). Before the film formation, all substrates were precleaned chemically and exposd to UV−ozone to eliminate residual impurities. The films were spin-coated at 2000 rpm for 60 s and dried in a glovebox on a hot plate at $T = 60$ °C for 1 h. The film thicknesses were ∼50 nm.

The absorption spectra of the films were recorded on an UV−vis−near-IR recording spectrophotometer UV-3100, Shimadzu. The emission (PL) spectra were measured using Spectrofluorometer FP-6500-A-51, Jasco.

Φ_f of the films was measured under nitrogen flow using an integrating sphere with a He−Cd laser ($\lambda = 325$ nm) as an excitation source and a multichannel spectrometer (Hamamatsu PMA-11) as an optical detector. The transient photoluminescence was measured using a streak camera (Hamamatsu C4334) with a nitrogen gas laser ($\lambda = 337$ nm, pulse width ∼ 300 ps, and repetition rate = 20 Hz) as an excitation source. The measurements were done under a low pressure (∼10^{-1} Pa) in a cryostat. The highest occupied molecular orbital (HOMO) level was measured with an ultraviolet photoelectron spectroscopy (AC-1, Riken Keiki Co.). The surface morphology of the films was observed using a scanning atomic force microscope (JEOL JSPM-5200) with a contact mode.

To understand characteristics of the molecular aggregation such as excimer formation, we measured PL characteristics of degassed solutions of the trimers in dichloromethane with the concentrations of 10^{-5} and 10^{-2} M, and their thin films formed by spin coating from a 10^{-2} M solution of DCM.

To investigate electroluminescence (EL) properties of the samples, an OLED structure of ITO/PEDOT:PSS/trimer/Mg:Ag/Ag was prepared as follows: a 70 nm thick layer of poly(ethylenedioxythiophene):poly(styrenesulfonic acid) (PEDOT:PSS) were spin-coated on precleaned ITO-coated (110 nm) glass substrates at 2000 rpm and dried in air on a hot plate at 200 °C for 10 min. Next, 1 wt % solutions of **OXD**, **TPA**, or **PYR** in dichloromethane were spin-coated at 2000 rpm at room temperature and dried in a glovebox on a hot plate at 60 °C for 1 h. A magnesium:silver (Mg:Ag) alloy layer (10:1) capped with a silver layer was deposited on top of the organic layers. The

SCHEME 1

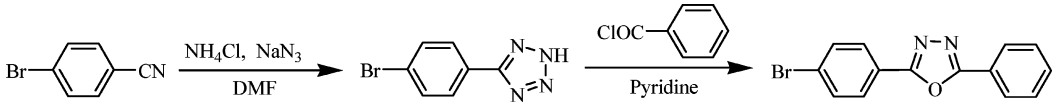

TABLE 1: Decomposition Temperatures, Glass Transition Temperatures, and Photophysical Properties of Trimers in THF Solution[a]

trimer	T_d[b] (°C)	Y_c[c] (%)	T_g[d] (°C)	$\lambda_{a,max}$[e] in solution (nm)	$\lambda_{f,max}$[f] in solution (nm)	Φ_f[g] in solution
OXD	385	38	33	379	455	0.71
TPA	433	64	60	389	471	0.65
PYR	430	56	52	395	*471*, 500	0.74

[a] Italicized numerical values denote absolute maxima. The PL emission spectra were measured using the corresponding excitation maximum as excitation wavelength. [b] Decomposition temperature corresponding to 5% weight loss in N_2 determined by TGA. [c] Char yield at 800 °C in N_2 determined by TGA. [d] Glass transition temperature determined by TMA. [e] $\lambda_{a,max}$: The absorption maximum from the UV−vis spectra in THF solution. [f] $\lambda_{f,max}$: The PL emission maximum in THF solution. [g] Φ_f: PL quantum yield relative to quinine sulfate in 1 N H_2SO_4.

TABLE 2: Absolute PL Efficiency Φ_f (%) of Trimers in DCM Solutions and in Thin Films[a]

	solution[b]		
trimer	10^{-5} M	10^{-2} M	film[c]
OXD	70	20	10
TPA	67	11	4
PYR	64	10	2

[a] Absolute PL efficiency Φ_f (%) determined using an integrating sphere. [b] In dichloromethane (DCM). [c] Spin-coated thin films from a 10^{-2} M DCM solution at 2000 rpm for 60 s and dried in a glovebox on a hot plate at 60 °C for 1 h.

current density−voltage−luminance ($J-V-L$) characteristics were measured using a semiconductor parameter analyzer (Agilent, HP4155C) with an optical power meter (Newport, Model 1835-C).

Reagents and Solvents. 2,7-Dibromofluorene[38] was synthesized according to a reported procedure. 2,7-Dibromo-9,9-dihexylfluorene was synthesized by the reaction of 2,7-dibromofluorene with 1-bromohexane, catalyzed by concentrated NaOH (aqueous 50% (w/w)), and in the presence of a phase-transfer catalyst, trimethylbenzylammonium chloride.[39] Dimethylformamide (DMF) was dried by distillation over CaH_2. Triethylamine was purified by distillation over KOH. All other reagents and solvents were commercially purchased and were used as supplied.

Preparation of Monomers. *9,9-Dihexyl-2,7-divinylfluorene (1).* Stille coupling reaction[40] was used to prepare compound **1**. A flask was charged with a mixture of 2,7-dibromo-9,9-dihexylfluorene (0.8129 g, 1.65 mmol), tributylvinyltin (1.15 g, 3.63 mmol), $PdCl_2(PPh_3)_2$ (0.0463 g, 0.07 mmol), a few crystals of 2,6-di-*tert*-butylphenol, and toluene (15 mL). The mixture was stirred and heated at 100 °C for 24 h under N_2. It was subsequently diluted with ether and treated with KF solution (∼10%). The resulting mixture was stirred for 20 h and followed by suction filtration to remove the insoluble solid. The organic layer was dried (Na_2SO_4) and concentrated. The concentrate was purified by column chromatography with *n*-hexane as eluent to afford compound **1** (0.56 g, yield 88%). FT-IR (KBr, cm^{-1}): 2956, 2928, 2856, 1628, 1604, 1468, 1400, 1376, 988, 902, 824, 748. ^{1}H NMR ($CDCl_3$, ppm): δ 7.62 (d, J = 7.8 Hz, 2H); 7.38 (m, 4H); 6.81 (dd, J_1 = 10.9 Hz, J_2 = 6.7 Hz, 2H); 5.81 (d, J = 17.6 Hz, 2H), 5.26 (d, J = 10.9 Hz, 2H); 1.96 (m, 4H); 1.04 (m, 16H); 0.76 (t, J = 6.9 Hz, 6H). ^{13}C NMR ($CDCl_3$, ppm): δ 151.84, 141.14, 137.43, 136.01, 125.26, 120.53, 119.70, 113.01, 55.26, 40.44, 31.50, 29.73, 23.72, 22.61, 14.02. Anal. Calcd for $C_{29}H_{38}$: C, 90.09; H, 9.91. Found: C, 89.54; H, 9.85.

4-Bromophenyltetrazole. A flask was charged with a mixture of 4-bromobenzonitrile (4.00 g, 21.9 mmol), NH_4Cl (18.80 g, 350.4 mmol), NaN_3 (22.85 g, 350.4 mmol), and DMF (80 mL). The mixture was refluxed for 3 days. It was subsequently cooled at room temperature and poured into dilute hydrochloric acid

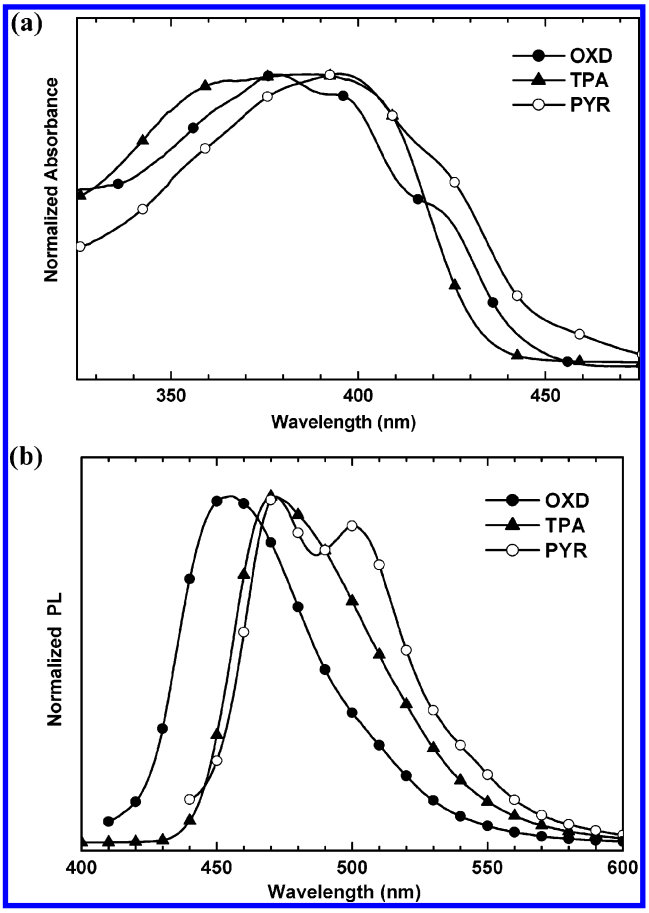

Figure 1. Normalized UV−vis absorption spectra (a) and PL emission spectra (b) of trimers in THF solution. The PL emission spectra were measured using the corresponding excitation maximum as excitation wavelength.

TABLE 3: HOMO Levels and Photophysical Properties of Trimer Films[a]

trimer	HOMO[b] (eV)	Φ_f[c] (%)	η_{EL}[d] (%)	$\lambda_{a,max}$[e] (nm)	$\lambda_{f,max}$[f] (nm)	$\lambda_{EL,max}$[g] (nm)	λ_{f1}[h] (nm)	λ_{f2}[h] (nm)	RMS[i] (nm)
OXD	5.52	9.94	0.02	383	*471*, 502	550	496	534	16.3
TPA	5.05	3.7	0.011	417	477, 510, *565*	*498*, 565, 630	491	587	50.6
PYR	5.75	1.9	4.3×10^{-5}	417	565		551	603	15.2

[a] Italicized numerical values denote the PL maxima. The PL emission spectra were measured using the corresponding excitation maximum. [b] Highest occupied molecular orbital (HOMO) level determined using AC-1. [c] Absolute PL efficiency determined using an integrating sphere. [d] Maximum EL quantum efficiency calculated from $J-V-L$ characteristics of ITO/PEDOT:PSS/trimer/Mg:Ag/Ag. [e] $\lambda_{a,max}$: The absorption maximum from the UV−vis spectra in the thin films formed from 1 wt % solution in DCM. [f] $\lambda_{f,max}$: The PL emission maximum in the thin films formed from 1 wt % solution in DCM. [g] $\lambda_{el,max}$: The EL emission maximum in the OLEDs. [h] λ_{f1}: The fast component of PL measured using a streak camera. λ_{f2}: The delayed component of PL measured using a streak camera. [i] RMS: The root-mean-square roughness of the film surfaces obtained from AFM measurements.

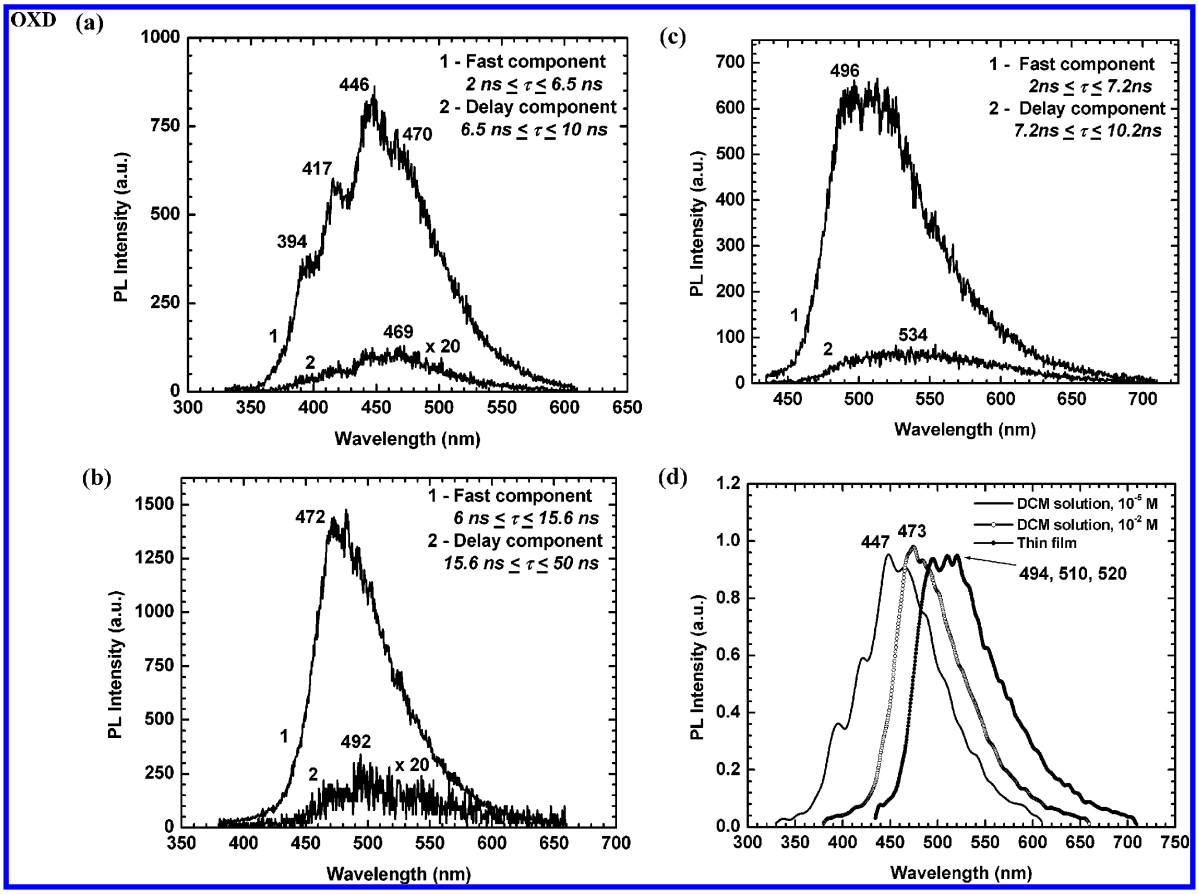

Figure 2. Fast and delayed component of PL spectra of **OXD** in 10^{-5} M (a) and 10^{-2} M DCM (b) solutions and thin film formed from a 10^{-2} M DCM solution (c). Comparative PL spectra of **OXD** in DCM solutions and in the thin film (d).

solution. The precipitate was filtered and washed thoroughly with water. The crude product was recrystallized from ethanol (1.52 g, yield 31%; mp 255−257°C (dec.)).

2-(4-Bromophenyl)-5-phenyl-1,3,4-oxadiazole. A mixture of 4-bromophenyltetrazole (1.46 g, 6.47 mmol), benzoyl chloride (1.45 g, 10.32 mmol), and pyridine (15 mL) was refluxed for 3 days under N_2 atmosphere. The solution was poured into water, and the solid was filtered, washed with water, and dried. The crude product was recrystallized from ethanol (1.61 g, yield 82%; mp 176−178 °C, lit.[41] 180 °C). The spectroscopic characterization of the product was in agreement with literature.[41]

Preparation of Trimers. The preparation of **OXD** is given as a typical example for the preparation of trimers. A flask was charged with a mixture of **1** (0.1999 g, 0.517 mmol), 2-(4-bromophenyl)-5-phenyl-1,3,4-oxadiazole (0.3114 g, 1.034 mmol), $Pd(OAc)_2$ (0.0023 g, 0.010 mmol), P(*o*-tolyl)$_3$ (0.0063 g, 0.021 mmol), DMF (8 mL), ant triethylamine (2 mL). The flask was degassed and purged with N_2. The mixture was heated at 90 °C for 24 h under N_2. Then, it was filtered, and the filtrate was poured into methanol. The yellow-green precipitate was filtered and washed with methanol. The crude product was purified by being dissolved in THF and precipitated into methanol (0.11 g, yield 26%). Anal. Calcd for $C_{57}H_{54}N_4O_2$: C, 82.78; H, 6.58; N, 6.77. Found: C, 81.93; H, 6.65; N, 6.68.

The trimers **TPA** and **PYR** were prepared in yields of 75 and 71%, respectively.

TPA. Anal. Calcd for $C_{65}H_{64}N_2$: C, 89.40; H, 7.39; N, 3.21. Found: C, 88.76; H, 7.35; N, 3.37.

PYR. Anal. Calcd for $C_{61}H_{54}$: C, 93.08; H, 6.92. Found: C, 92.65; H, 6.74.

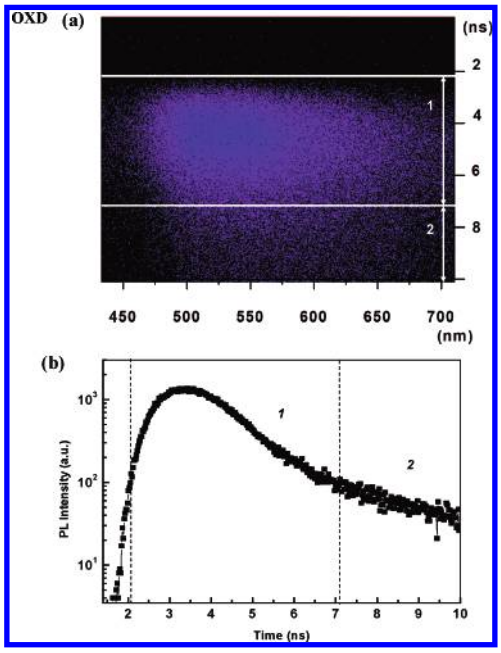

Figure 3. Streak camera images of PL spectra in **OXD** thin film formed from a 10^{-2} M DCM solution (a) and the corresponding double-exponential decay curve (b) showing the fast (1) and delayed (2) components.

Results and Discussion

Synthesis and Characterization. Starting from 9,9-dihexyl-2,7-divinylfluorene (**1**), three novel trimers were synthesized via Heck coupling.[42] In particular, **1** reacted with appropriate bromides in a molar ratio of 1:2 utilizing DMF as reaction

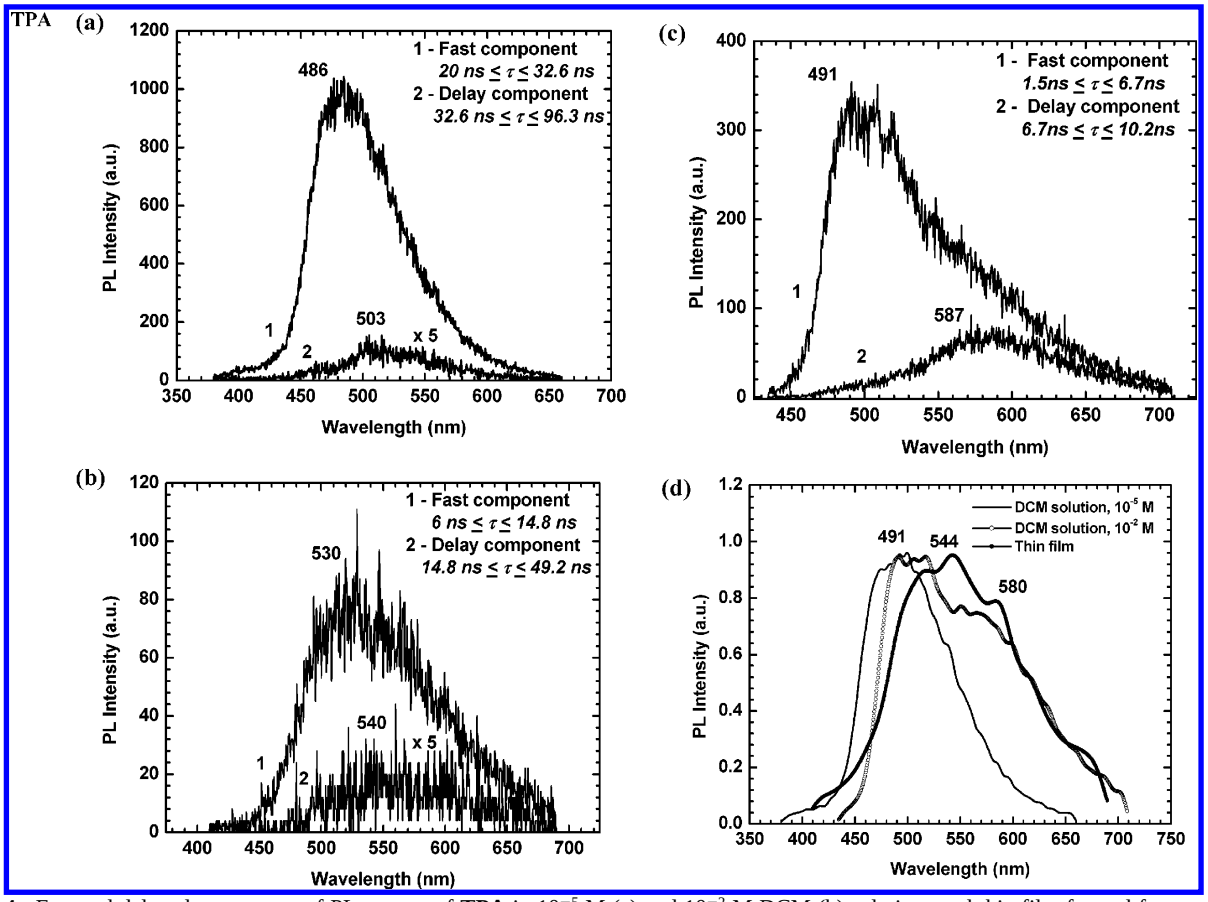

Figure 4. Fast and delayed component of PL spectra of **TPA** in 10^{-5} M (a) and 10^{-2} M DCM (b) solutions and thin film formed from a 10^{-2} M DCM solution (c). Comparative PL spectra of **TPA** in DCM solutions and in the thin film (d).

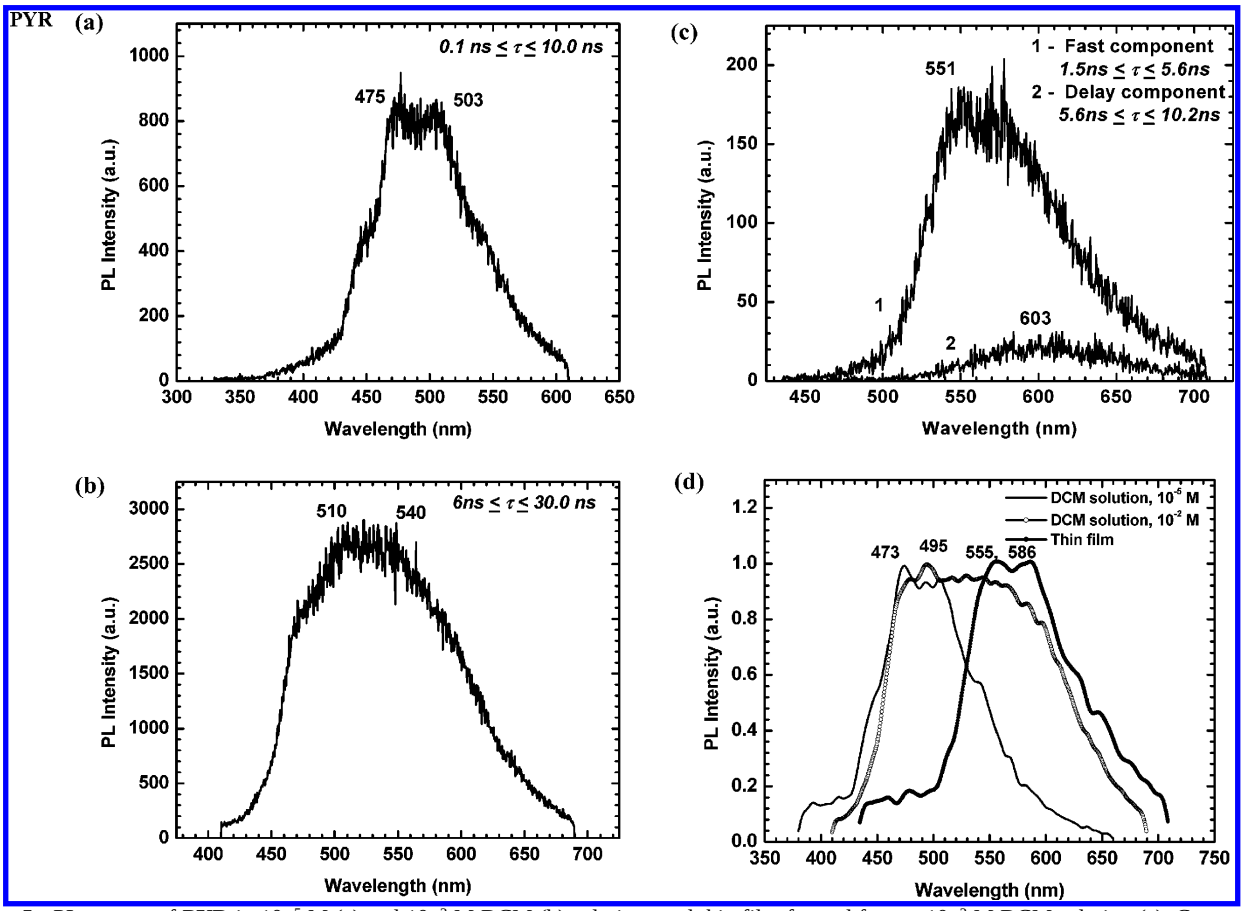

Figure 5. PL spectra of **PYR** in 10^{-5} M (a) and 10^{-2} M DCM (b) solutions and thin film formed from a 10^{-2} M DCM solution (c). Comparative PL spectra of **PYR** in DCM solutions and in the thin film (d).

medium and triethylamine as an acid acceptor. The following bromides were used as reactants for the Heck reaction with **1**: 2-(4-Bromophenyl)-5-phenyl-1,3,4-oxadiazole,[41] *N*,*N*-diphenyl-4-bromoaniline,[43] and 3-bromopyrene[44] to afford the trimers **OXD**, **TPA,** and **PYR**, respectively (Chart 1). These bromides were synthesized according to reported methods. Scheme 1 outlines the synthesis of 2-(4-bromophenyl)-5-phenyl-1,3,4-oxadiazole.[41] Specifically, 4-bromobenzonitrile reacted with a mixture of NH_4Cl and NaN_3 in DMF to afford 4-bromophenyl-tetrazole. The latter reacted subsequently with benzoyl chloride in pyridine to yield the target bromide.

Trimers **OXD**, **TPA**, and **PYR** were isolated by pouring the reaction mixture into methanol, and they were purified by dissolving in THF and precipitating with methanol. The preparation yields ranged from 26 to 75%. These trimers were readily soluble in common organic solvents such as THF, dichloromethane, chloroform, and toluene. Their molecular structures were identified by FT-IR and ^{1}H NMR spectroscopy. The FT-IR spectra showed common characteristic absorption bands around 2926, 2850 (C−H stretching of aliphatic moieties); 3028, 1600, 1490, 1464 (aromatic); and 960 cm^{-1} (trans olefinic bond). In addition, **TPA** displayed absorptions at 1328 and 1344 cm^{-1} assigned to the C−N stretching of the triphenylamine units. Finally, the absorptions at 1488 and 1070 cm^{-1} of **OXD** are associated with the oxadiazole ring. All the ^{1}H NMR spectra exhibited resonances at about 8.30−7.00 (aromatic and olefinic protons); 2.00 [$CH_2(CH_2)_4CH_3$]; 1.20 [$CH_2(CH_2)_4CH_3$]; and 0.80 ppm [$CH_2(CH_2)_4CH_3$]. **OXD** showed a characteristic multiplet at 8.17 ppm assigned to the eight aromatic protons ortho to oxadiazole rings. Even though it is difficult to distinguish the aromatic from the olefinic protons, the ^{1}H NMR spectra of the trimers suggested the formation of trans olefinic bonds from the Heck reaction since they lacked entirely a peak of cis olefinic protons near 6.50 ppm. This feature is in line with the IR absorption around 960 cm^{-1} that confirmed the trans olefinc bonds.

The thermal and thermomechanical characterization of trimers was accomplished by TGA and TMA. The decomposition temperature (T_d), corresponding to a weight loss of 5%, and the char yield (Y_c) in N_2 are listed in Table 1. No weight loss was observed up to about 250 °C for **OXD** and up to 350 °C for **PYR** and **TPA**. On the basis of the T_d and Y_c the thermal stability of trimers was of the order **OXD** < **PYR** < **TPA**. The glass transition temperatures (T_g's) of trimers, which were determined by TMA using a loaded penetration probe, followed the same trend (Table 1). They were obtained from the onset temperature of the baseline shift recorded during the second heating. The T_g values were relatively low (33−60 °C), indicating the suppressed rigidity of trimers. T_g's of 73−114 °C have been reported for 2,7-linked 9,9-diisobutylfluorene trimers.[45]

Photophysical Properties. The photophysical properties of the trimers were investigated both in dilute THF and DCM solutions and in their thin film, which are summarized in Tables 1−3, respectively.

The trimers emitted blue-green light with PL maximum at $\lambda_{f,max}$ = 455−500 nm in THF solution and $\lambda_{f,max}$ = 471−565 nm in the thin films (Figures 1−6). The $\lambda_{f,max}$ of **OXD** was blue-shifted by 16−94 nm relative to those of **TPA** and **PYR** due to the presence of the electron-deficient oxadiazole ring in the former. The **PYR** emission spectrum in THF solution showed a typical vibronic progression with emission bands located at 471 and 500 nm. **PYR** thin film displayed $\lambda_{f,max}$ at 565 nm, which is significantly red-shifted as compared to

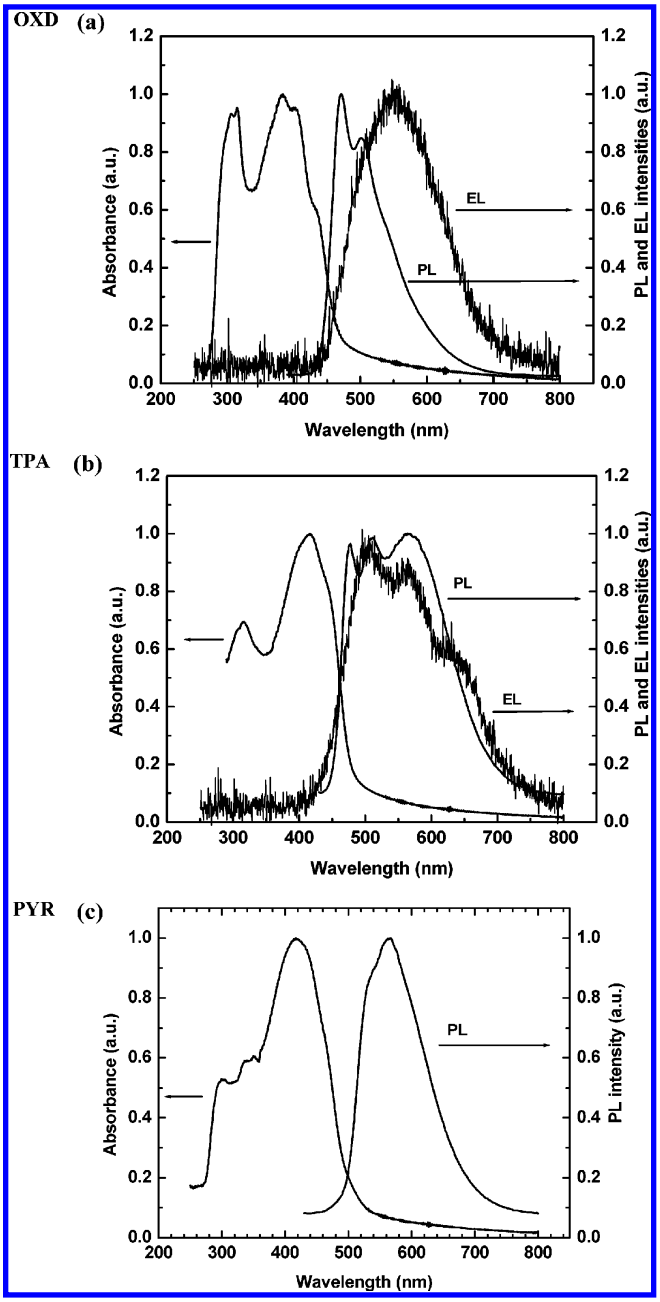

Figure 6. Absorption, PL, and EL spectra of **OXD** (a), **TPA** (b), and **PYR** (c) in their thin films. The EL spectra in the OLED structures of ITO/PEDOT:PSS/trimer/Mg:Ag/Ag were measured at current density of J = 200 mA/cm^2.

solution due to the strong tendency of pyrene to form excimers.[33,48] Generally, the emission of these trimers is red-shifted as compared to poly(9,9-dihexylfluorene)[49] (415−422 nm), and it is comparable to poly(9,9-dioctylfluorene-2,7-vinylene)[47] (507 nm).

The emission efficiency of the trimers was evaluated by determination[50] of their Φ_f in THF solution using quinine sulfate as standard (Table 1). They showed high emission efficiency since their Φ_f values ranged from 0.65 to 0.74.

The optical band gaps (E_g) of the trimers, **OXD**, **TPA**, and **PYR**, calculated from the onset of the absorption spectra in their thin film were 2.66, 2.59, and 2.47 eV, respectively. The E_g is 2.9 eV for poly(9,9-dihexylfluorene)[46] and 2.6 eV for poly-(9,9-dioctylfluorene-2,7-vinylene).[47]

The HOMO levels of **PYR**, **OXD**, and **TPA** thin films were I_p = 5.75, 5.52, and 5.05 eV (Table 3), respectively. These

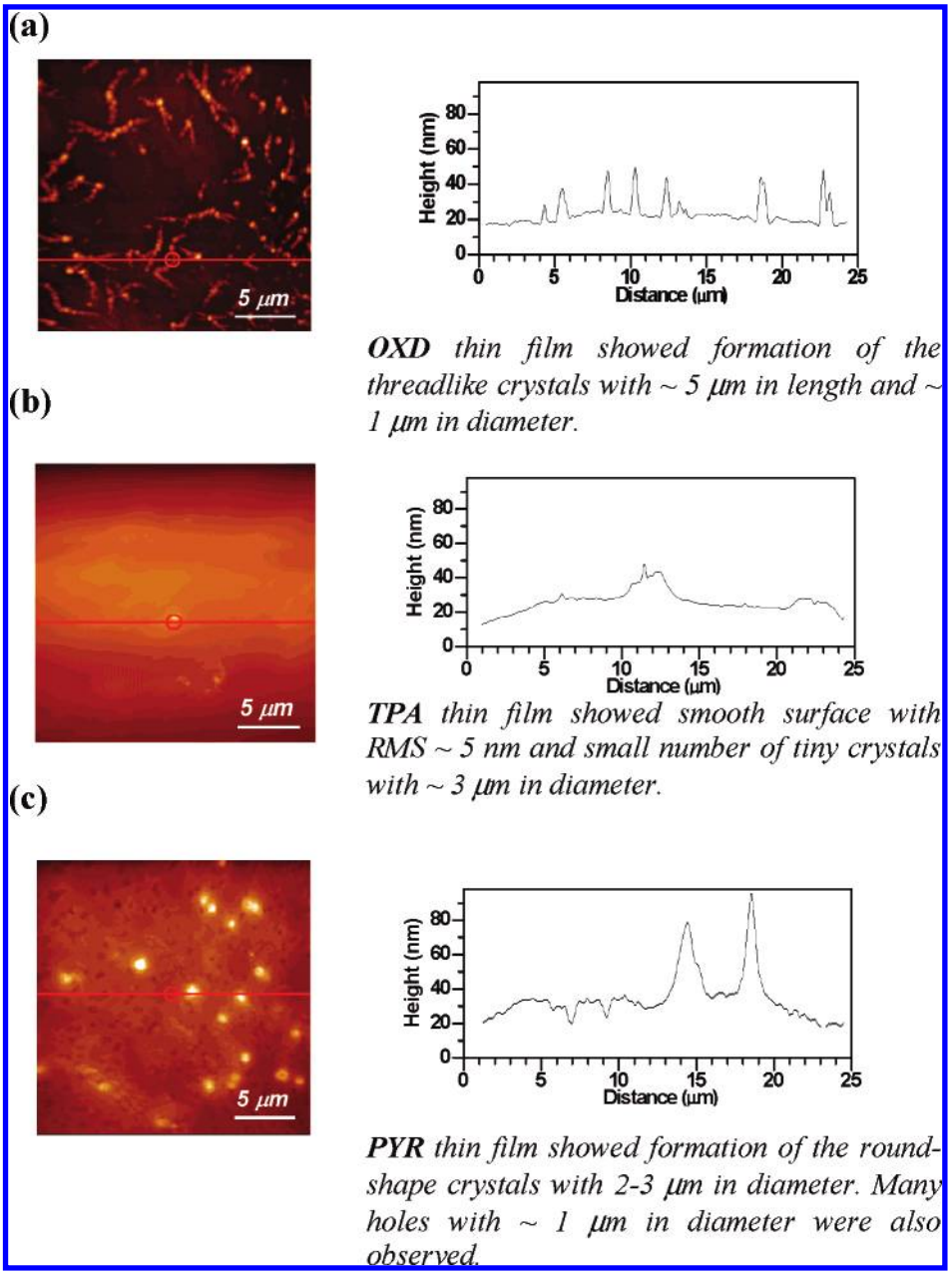

Figure 7. AFM image (topography) of **OXD** (a), **TPA** (b), and **PYR** (c) thin films on a Si substrate. The image size is 25 μm × 25 μm.

values are well-correlated to the donor and acceptor nature of the substituents. The **PYR** film showed the deepest I_p due to the presence of extended π-conjugated pyrene groups, while the **TPA** having electron-donating groups showed the highest I_p. The **OXD** having electron-withdrawing groups showed the intermediate I_p value between the I_p of **PYR** and **TPA**.

OXD, **TPA**, and **PYR** showed strong concentration dependence in Φ_f (Tables 2 and 3). All materials have relatively high PL efficiency of $\Phi_f = 64-70\%$ in a diluted DCM solution (10^{-5} M), while the PL efficiencies of the thin films were significantly lower than those in solution, resulting in $\Phi_f = 2-10\%$. This is due to the strong PL quenching caused by molecular aggregation such as excimer formation.[33,48,51,52] Transient PL measurement showed that both the solution and thin film have a nanosecond PL lifetime. The PL spectra, as shown in Figures 2−5, clearly indicate presence of two components for all films in which the delayed component suggests the excimer formation.[48] The ratios of integrated PL intensities of the prompt and delayed components are 9, 5, and 4 for **OXD**, **TPA**, and **PYR**. On the other hand, the diluted DCM solutions (10^{-5} M) of all trimers showed no significant delayed components corresponded to the excimer emission. Furthermore, with an increase of the concentration up to 10^{-2} M, the appreciable delayed emission of **TPA** and **OXD** appeared. In addition, comparing PL spectra of both solutions and thin film for the trimers (Figures 2d (**OXD**), 4d (**TPA**), and 5d (**PYR**)), the formation of the molecular aggregation is evident.

In the case of **OXD**, with an increase of the solution concentration, the long wavelength shift in the PL spectrum was observed (Figure 2). The PL lifetimes of **OXD** in 10^{-5} and 10^{-2} M solutions were $\tau = 1.2$ ns and $\tau = 1.6$ ns, respectively. Furthermore, in the film, the red shift of the PL spectrum and two components of $\tau = 1.1$ ns and $\tau = 3.6$ ns were observed, indicating excimer formation (Figure 3).

With an increase of **TPA** concentration in a DCM solution from 10^{-5} to 10^{-2} M, the red shift and broadening of the PL spectra with the PL lifetime of $\tau = 1.7$ ns for 10^{-5} M and $\tau = 2.1$ ns for 10^{-2} M, respectively, were observed (Figure 4). The

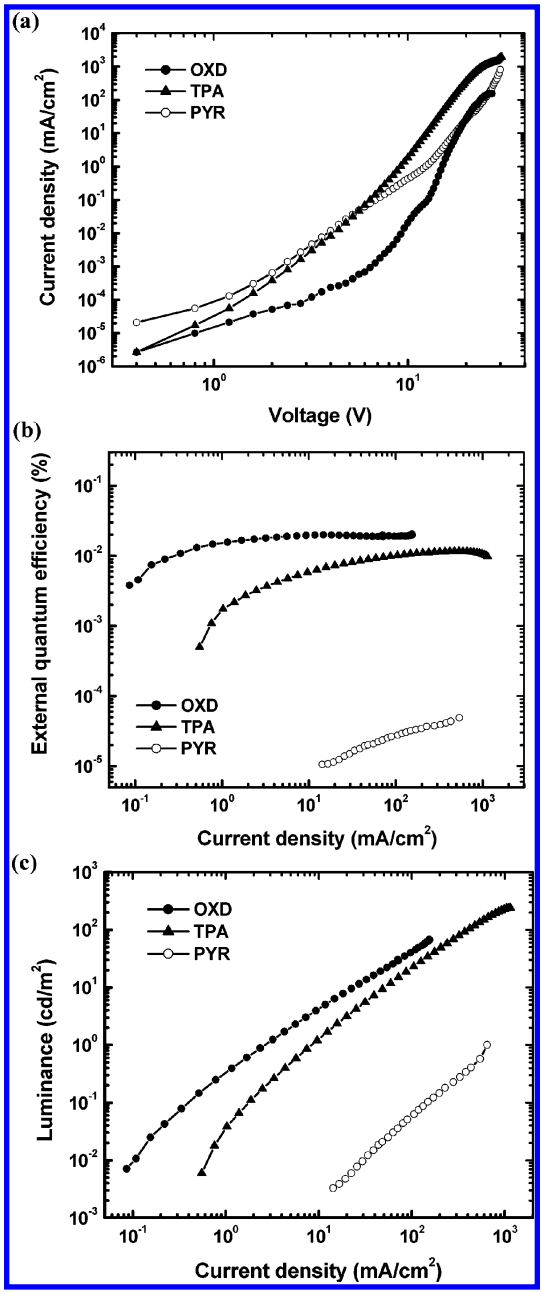

Figure 8. Current density−voltage ($J-V$) (a), EL quantum efficiency vs current density ($\eta_{EL}-J$) (b), and luminance−current density ($L-J$) (c) characteristics of ITO/PEDOT:PSS/trimer/Mg:Ag/Ag devices with **OXD**, **TPA**, and **PYR** as an active layer.

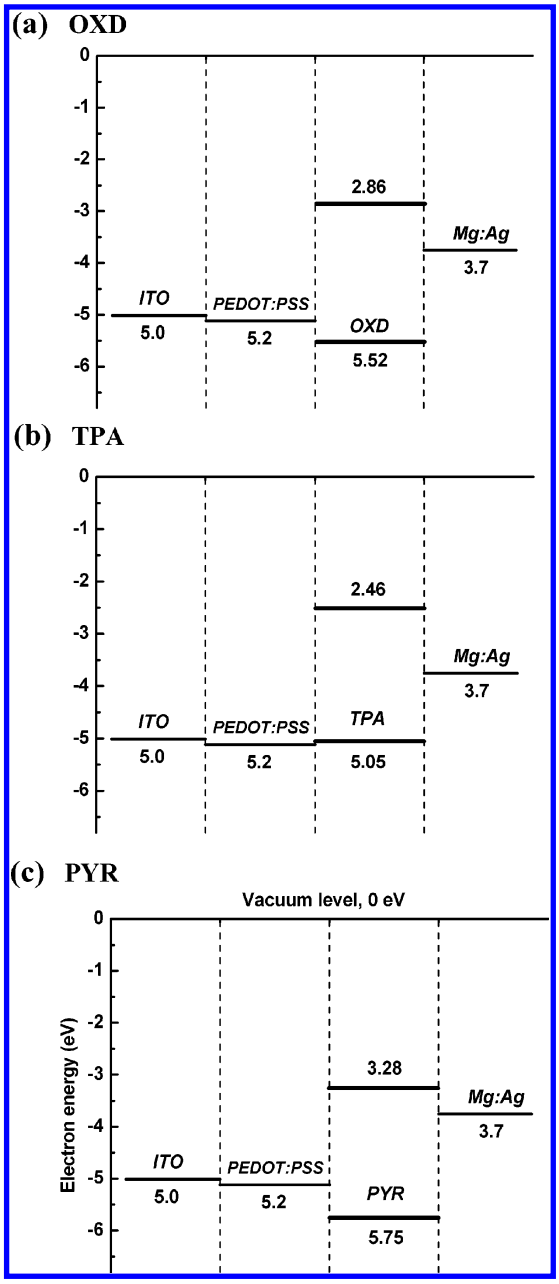

Figure 9. Energetic diagrams of ITO/PEDOT:PSS/trimer/Mg:Ag/Ag devices with **OXD** (a), **TPA** (b), and **PYR** (c) as an active layer.

neat film showed a red shift of PL maxima and two components of PL lifetime ($\tau = 1.3$ ns and $\tau = 3.1$ ns), indicating an excimer formation.

In the case of **PYR**, the 10^{-2} M solution in DCM showed a PL spectrum with red shift of maximum and significant broadening compared with that in the solution of 10^{-5} M (Figure 5). Such broadening of the PL spectrum and an increase of transient lifetime from $\tau = 1.5$ ns in the 10^{-5} M solution to $\tau = 2.1$ ns in the 10^{-2} M solution suggest the presence of the excimer emission. The PL spectrum of the neat film also showed the longer red shift of PL maxima and two components of PL lifetime ($\tau = 0.9$ ns and $\tau = 2.1$ ns), indicating the excimer formation.

The propensity of the molecular aggregation was also confirmed with the atomic force microscopy (AFM) investigation, as shown in Figure 7. The **OXD** films showed formation of the threadlike crystals with ~5 μm in length and ~1 μm in diameter (Figure 7a). **TPA** almost formed a smooth layer with root mean square (RMS) of a few nanometers and a very small number of microcrystals on the film surface. The surface morphology of a **PYR** layer is inferior due to the presence of various round-shaped crystals with 2−3 μm in diameter and holes.

EL Device Properties. The OLED structures of ITO/PEDOT:PSS/trimer/Mg:Ag/Ag were fabricated. Figure 6 shows the EL spectra of these devices as well as the UV−vis absorption and the PL emission spectra of trimer thin films. Figure 8 shows the current density−voltage (a), the external EL quantum efficiency−current density (b), and the luminance−current density characteristics of the devices. The OLEDs displayed green EL with brightness of up to ~240 cd/m^2.

The OLED with **OXD** as an emitting layer showed green emission with maximum at $\lambda_{EL,max} \sim 550$ nm and $\eta_{EL} \sim 0.02\%$ at 15 V. The maximum luminance of ~68 cd/m^2 was obtained at $J = 130$ mA/cm^2 and applied voltage of 26 V (Figure 8). The luminance at $J = 100$ mA/cm^2 and 22 V was ~40 cd/m^2.

The EL emission peak was shifted to longer wavelength region of 80 nm compared with the PL maximum, suggesting that the EL emission selectively occurs at the excimers sites. Since **OXD** contains oxadiazole units which have high electron transport ability, the electron injection and transport should be improved compared with those of **TPA** and **PYR**, leading to the highest η_{EL} in the trimers. The hole and electron injection barriers into the **OXD** layer from the adjacent layers estimated from the energetic diagram (Figure 9a) were ∼0.32 and ∼0.84 eV, respectively. The improved electron transport ability of **OXD** and rather small electron injection barrier promote improvement of the carrier balance.

The OLED device with **TPA** as an active layer showed green emission with the main maximum at $\lambda_{EL,max} \sim 498$ nm and subpeaks at ∼565 and ∼630 nm, which are approximately coincided with the PL spectrum. The maximum of η_{EL} was ∼0.01 % at 14 V, and the maximum luminance of ∼240 cd/m^2 was observed at $J = 1.1$ A/cm^2 and applied voltage of 22 V (Figure 8). The luminance at $J = 100$ mA/cm^2 and 14 V was ∼21 cd/m^2. As estimated from the energetic diagram shown in Figure 9b, although **TPD** has virtually no injection barrier for holes, a high energy barrier for electron injection (∼1.31 eV) was identified. In addition, since the triphenylamine unit has an excellent hole transporting ability, the unbalanced carrier injection and transport would lead to high driving voltage and low η_{EL}. Another factor for low η_{EL} is due to quenching of excitons by the molecular aggregation and excimer formation.

Very poor EL characteristics were observed in the OLED device with **PYR**. η_{EL} was $\sim 4.3 \times 10^{-5}$% at 30 V. The maximum luminance of ∼1 cd/m^2 was obtained at current density of ∼600 mA/cm^2 and applied voltage of 30 V (Figure 8). Due to the low η_{EL}, it was difficult to measure the EL spectrum. The luminance at $J = 100$ mA/cm^2 and 23 V was ∼0.06 cd/m^2. From the energetic diagram shown in Figure 9c, we estimated the hole and electron injection barriers as 0.55 and 0.42 eV, respectively. Since the estimated energy barrier for hole injection is rather high, we can assume that unbalanced hole and electron injection possibly results in low η_{EL}. Further, the interior film quality of the **PYR** layer (Figure 7c) would also lead to low η_{EL}.

Conclusions

The Heck reaction of 9,9-dihexyl-2,7-divinylfluorene with appropriate bromides afforded three new soluble 2,7-fluorene-vinylene-based trimers **OXD**, **TPA**, and **PYR**, which contained oxadiazole, triphenylamine, and pyrene segments, respectively. All trimers possessed thermal stabilities of more than 250−350 °C and displayed relatively low T_g values (33−60 °C). They also absorbed light in the range of 379−417 nm and had optical band gaps of 2.47−2.66 eV. Their light emission was blue-green in both solution and solid state with PL maximum at the range of 455−565 nm and quantum yields of 0.65−0.74 in THF solution. All samples were fluorescent and showed nanosecond lifetime with two components in the neat films. The presence of delayed component was ascribed to the formation of excimers. The OLED structures with **OXD** and **TPA** showed green emission with EL quantum efficiency of $\eta_{EL} \sim 10^{-2}$%, while very low EL efficiency ($\sim 4.3 \times 10^{-5}$%) was observed in **PYR**. **OXD**, **TPA**, and **PYR** showed the propensity to the excimer formation and concentration quenching, leading to low emission efficiency.

Supporting Information Available: Figures showing the FT-IR and ^{1}H NMR spectra as well as the TGA and TMA traces of trimers **OXD**, **TPA**, and **PYR**. This material is available free of charge via the Internet at http://pubs.acs.org.

References and Notes

(1) Dimitrakopoulos, C. D.; Malenfant, P. R. L. *Adv. Mater.* **2002**, *14*, 99.
(2) Katz, H. E.; Bao, Z. *J. Phys. Chem. B* **2000**, *104*, 671.
(3) Horowitz, G. *Adv. Mater.* **1998**, *10*, 365.
(4) Brabec, C. J.; Sariciftci, N. S.; Hummelen, J. C. *Adv. Funct. Mater.* **2002**, *12*, 192.
(5) Sariciftci, N. S.; Braun, D.; Zhang, C.; Srdanov, V. I.; Heeger, A. J.; Stucky, G.; Wudl, F. *Appl. Phys. Lett.* **1993**, *62*, 585.
(6) Neher, D. *Macromol. Rapid Commun.* **2001**, *22*, 1365.
(7) Leclerc, M. *J. Polym. Sci., Part A: Polym. Chem.* **2001**, *39*, 2867.
(8) Mitschke, U.; Bauerle, P. *J. Mater. Chem.* **2000**, *10*, 1471.
(9) Kraft, A.; Grimsdale, A. C.; Holmes, A. B. *Angew. Chem., Int. Ed.* **1998**, *37*, 402.
(10) Burroughes, J. H.; Bradley, D. D. C.; Brown, A. R.; Marks, R. N.; MacKay, K.; Friend, R. H.; Burns, P. L.; Holmes, A. B. *Nature* **1990**, *347*, 539.
(11) Gruber, J.; Li, R. W. C.; Hümmelgen, I. A. In *Handbook of Advanced Electronic and Photonic Materials and Devices*; Nalwa, H. S., Ed.; Academic Press: San Diego, 2001; Vol. 8, p 163.
(12) Ohmori, Y.; Uchida, M.; Muro K.; Yoshino, K. *Jpn. J. Appl. Phys., Part 2* **1991**, *30*, 1941.
(13) Pei Q.; Yang, Y. *J. Am. Chem. Soc.* **1996**, *118*, 7416.
(14) Cho, H. N.; Kim, D. Y.; Lee J. Y.; Kim, C. Y. *Adv. Mater. (Weinheim, Ger.)* **1997**, *9*, 326.
(15) Ranger, M.; Rondeau D.; Leclerc, M. *Macromolecules* **1997**, *30*, 7686.
(16) Grice, A.; Bradley, D. D. C.; Bernius, M. T.; Inbasekaran, M.; Wu W. W.; Woo, E. P. *Appl. Phys. Lett.* **1998**, *73*, 629.
(17) Stoessel, M.; Wittmann, G.; Staudigel, J.; Steuber, F.; Blässing, J.; Roth, W.; Klausmann, H.; Rogler, W.; Simmerer, J.; Winnacker, A.; Inbasekaran M.; Woo, E. P. *J. Appl. Phys.* **2000**, *87*, 4467.
(18) Sainova, D.; Miteva, T.; Nothofer, H. G.; Scherf, U.; Glowacki, I.; Ulanski, J.; Fugikawa H.; Neher, D. *Appl. Phys. Lett.* **2000**, *76*, 1810.
(19) Campbell, A. J.; Bradley, D. D. C.; Virgill, T.; Lidzey D. G.; Antoniadis, H. *Appl. Phys. Lett.* **2001**, *79*, 3872.
(20) Lupton, J. M.; Craig M. R.; Meijer, E. W. *Appl. Phys. Lett.* **2002**, *80*, 4489.
(21) Tang, H. Z.; Fujiki M.; Motonaga, M. *Polymer* **2002**, *43*, 6213.
(22) Fung, M. K.; Lai, S. L.; Tong, S. W.; Chan, M. Y.; Lee, C. S.; Lee, S. T.; Wu, W. W.; Inbasekaran M.; O'Brien, J. J. *Appl. Phys. Lett.* **2002**, *81*, 1497.
(23) Kulkarni A. P.; Jenekhe, S. A. *Macromolecules* **2003**, *26*, 5285.
(24) List, E. J. W.; Guentner, R.; de Freitas P. S.; Scherf, U. *Adv. Mater.* **2002**, *14*, 374.
(25) Kulkarni, A. P.; Kong X.; Jenekhe, S. A. *J. Phys. Chem. B* **2004**, *108*, 8689.
(26) Bliznyuk, V. N.; Carter, S. A.; Scott, J. C.; Klärner, G.; Miller, R. D.; Miller, D. C. *Macromolecules* **1999**, *32*, 361.
(27) Zojer, E.; Pogantsch, A.; Hennebicq, E.; Beljonne, D.; Brédas, J.-L.; Scandiucci de Freitas, P.; Scherf, U.; List, E. J. W. *J. Chem. Phys.* **2002**, *117*, 6794.
(28) Adachi, C.; Tsutsui, T.; Saito, S. *Appl. Phys. Lett.* **1989**, *55*, 1489.
(29) Schultz, B.; Bruma M.; Brehmer, L. *Adv. Mater.* **1997**, *9*, 601.
(30) (a) Thelakkat M.; Schmidt, H.-W. *Polym. Adv. Technol.* **1998**, *9*, 429. (b) Chondroudis K.; Mitzi, D. B. *Chem. Mater.* **1999**, *11*, 3028. (c) Wang, C.; Jung, G.-Y.; Batsanov, A. S.; Bryce M. R.; Petty, M. C. *J. Mater. Chem.* **2002**, *12*, 173. (d) Cha, S. W.; Choi, S.-H.; Kim; K.; Jin, K. J.-I. *J. Mater. Chem.* **2003**, *13*, 1900. (e) Kulkarni, A. P.; Tonzola, C. J.; Babel, A.; Jenekhe, S. A. *Chem. Mater.* **2004**, *16*, 4556.
(31) Stolka, M.; Yanus, J. F.; Pai, D. M. *J. Phys. Chem.* **1984**, *88*, 4707.
(32) Staudigel, J.; Stössel, M.; Steuber, F.; Simmerer, J. *J. Appl. Phys.* **1999**, *86*, 3895.
(33) Winnik, M. A.; Bystryak, S. M.; Liu, Z.; Siddiqui J. *Macromolecules* **1998**, *31*, 6855.
(34) (a) Arora, K. S.; Overberger, C. G.; Johnson, G. E. *J. Polym. Sci., Part B: Polym. Phys.* 1986, 24 2275. (b) Winnik, M. A.; Bystryak, S. M.; Liu, Z.; Siddiqui, J. *Macromolecules* **1998**, *31*, 6855. (c) Yyprachticky, D.; Cimrova V. *Macromolecules* **2002**, *35*, 3463.
(35) Oertel, U.; Appelhans, D.; Friedel, P.; Jehnichen, D.; Komber, H.; Pilch, B.; Hänel, B.; Voit, B. *Langmuir* **2002**, *18*, 105.
(36) Mikroyannidis, J. A.; Persephonis, P. G.; Giannetas, V. G. *Synt. Met.* **2005**, 148, 293.
(37) Mikroyannidis, J. A. *Synt. Met.* **2005**, *155*, 125.
(38) Yang, J.; Jiang, C.; Zhang, Y.; Yang, R.; Yang, W.; Hou, Q.; Cao, Y. *Macromolecules* **2004**, *37*, 1211.
(39) Lee, J. K.; Klaerner, G.; Miller, R. D. *Chem. Mater.* **1997**, *11*, 1083.
(40) McKean, D. R.; Parrinello, G.; Renaldo, A. F.; Stille, J. K. *J. Org. Chem.* **1987**, *52*, 422.

(41) Hou, S.; Chan, W. K. *Macromolecules* **2002**, *35*, 850.
(42) Ziegler, C. B.; Heck, R. F. *J. Org. Chem.* **1978**, *43*, 2941.
(43) Bacher, E.; Bayerl, M.; Rudati, P.; Reckefuss, N.; Müller, D.; Meerholz, K.; Nuyken, O. *Macromolecules* **2005**, *38*, 1640.
(44) *Organic Syntheses*; John Wiley and Sons: New York, 1973; Coll. Vol. 5, p 147.
(45) Sonntag, M.; Strohriegl, P. *Chem. Mater.* **2004**, *16*, 4736.
(46) Fakuda, M.; Sawada, K.; Yoshino, K. *Jpn. J. Appl. Phys.* **1989**, *28*, L1433.
(47) Jin, S.-H.; Park, H.-J.; Kim, J. Y.; Lee, K.; Lee, S.-P.; Moon, D.-K.; Lee, H.-J.; Gal, Y.-S. *Macromolecules* **2002**, *35*, 7532.
(48) (a) Blatchford, J. W.; Jessen, S.-B.; Lin, L.-B.; Gustafson, T. L.; Fu, D.-K.; Wang, H.-L.; M.; Swager, T. M.; MacDiarmid, A. G.; Epstein, A. *J. Phys. Rev. B* **1996**, *54*, 9180. (b) Jenekhe, S. A.; Osaheni, J. A. *Science* **1994**, *265*, 765.
(49) Liu, B.; Yu, W.-L.; Lai, Y.-H.; Huang, W. *Chem. Mater.* **2001**, *13*, 1984.
(50) Demas, J. N.; Crosby, G. A. *J. Phys. Chem.* **1971**, *75*, 991.
(51) Lee, J.-I.; Lee, V. Y.; Miller, R. D. *ETRI J.* **2002**, *24*, 409.
(52) Cimrova, V.; Hlidkova, H.; Vyprachticky, D.; Karastatiris, P.; Spiliopoulos, I. K.; Mikroyannidis, J. A. *J. Polym. Sci. B* **2006**, *44*, 524.